27 June 1969, Volume 164, Number 3887 SCIENCE

CURRENT PROBLEMS IN RESEARCH

New Detectors for High-Energy Physics

A total absorption technique is developed for the detection of electromagnetic and strongly interacting particles.

Robert Hofstadter

A principal motivation of this work is the belief that a major aspect of elementary particle physics in the future will be concerned with the appearance and explanation of sharp resonances and sharp spectral lines. Just as the study of the Balmer lines led to an understanding of atomic structure, and the study of nuclear gamma rays led to a clarification of nuclear structure, so it may be anticipated that spectroscopic investigations of high-energy gamma radiation will provide important clues to elementary particle structure. With this expectation in mind, the original idea of this research was aimed at the development of a new precise instrument for the detection of gamma radiation in the energy range 50 to 20,000 million electron volts.

In the course of this development, it soon became apparent that there was virtually no limit to the highest energy detectable and no restriction on the kind of radiation or particle which could be detected so long as one used the "total absorption principle." As far as I know, the first application of this principle to high-energy physics was made by Kantz and Hofstadter (*1*), although the total absorption method had been introduced earlier for the detection of gamma rays in sodium iodide (thallium) NaI(Tl) scintillation crystals by McIntyre and Hofstadter (*2*) in the energy range up to a few million electron volts.

Subsequent work on the total absorption spectrometry of gamma rays, electrons, and positrons detected by scintillation counters [for example, NaI(Tl)] and Cerenkov counters (for example, PbF_2) (*3*) was reported by Hofstadter (*4*). Berezin, Hofstadter, and Yearian (*5*) later investigated large NaI(Tl) scintillation counters as potential detectors of pions and showed that pions could be distinguished from electrons (and gamma rays).

A renewed interest in total absorption Cerenkov counters and scintillation counters developed after the recent application of these detectors to electromagnetic radiations in the energy range up to 14 Bev (*6–8*). Finally, the use of total absorption scintillation, Cerenkov, and conduction-type materials for the detection of strongly interacting particles and radiations was pointed out by Hofstadter (*9, 10*) in 1968.

An approximation to the total absorption method for the detection of strongly interacting particles has been developed by Grigorov, Murzin, Rapaport (*11*), Murzin (*12*), and Ramana Murthy, Sreekantan, Subramanian, and Verma (*13*). The device used by Grigorov and others has been called a "calorimeter." Since the calorimeter is essentially a sampling device in which a large fraction of the energy of the detected particles goes into nonsignal-producing energy-absorbing materials, I shall not discuss this type of detector any further. Variations of this same device (lead-lucite and lead-scintillator combinations) have been developed for detection of photons and electrons and are called "sandwich" counters. Some recent sandwich detectors are described by Heusch (*14*).

The author is professor in the department of physics and director of the High Energy Physics Laboratory of Stanford University, Stanford, California 94305.

Detector Principles, Characteristics, and Performance

TASC detectors for "electromagnetic" or Type A particles. For subsequent use we will classify the various particle types as indicated in Table 1. In this section and the next I will consider particles of type A. The detection of type B particles will be discussed below (*15*).

The total absorption technique can be illustrated by a consideration of very low energies, namely, the 1.17- and 1.33-Mev gamma radiations from Co^{60}. Figure 1 shows a scintillation pulse height spectrum observed in 1950 (*2*) in a NaI(Tl) crystal of volume 1 cm^3. The two peaks to the right are the total absorption peaks of the 1.17- and 1.33-Mev gamma rays of Co^{60}. The large peak on the left is a

Table 1. Types of high-energy particles.

Particles	Characteristics	Type of counter
	Type A	
e^-, e^+, γ	Produce electromagnetic showers	Total absorption shower cascade
	Type B	
n, $\bar{n}$, p, $\bar{p}$, π^+, π^-, K^+, K^-, K°, d, α, and so forth	Involve strong (nuclear) interaction	Total absorption nuclear cascade
	Type C	
ν, $\bar{\nu}$, μ^+, μ^-	Weakly interacting particles	

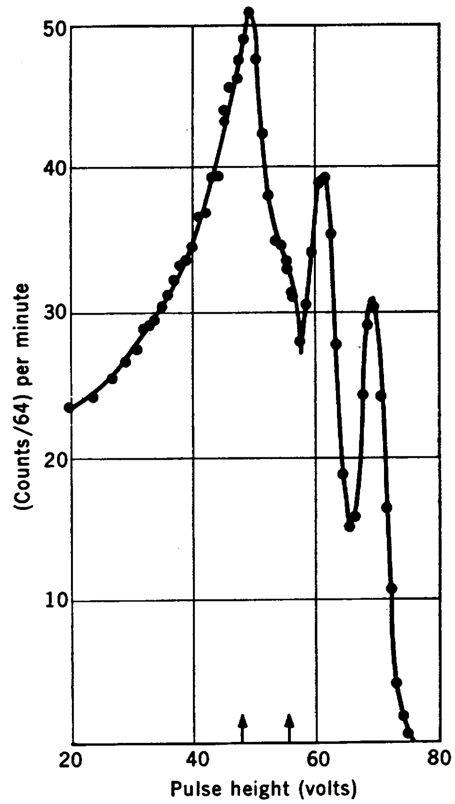

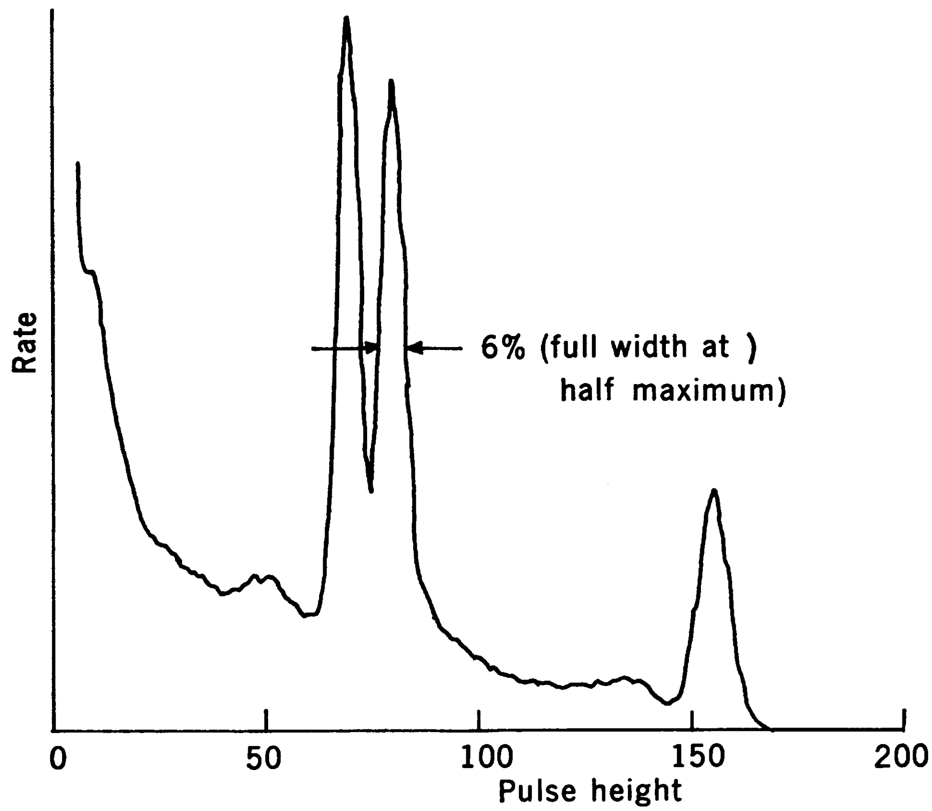

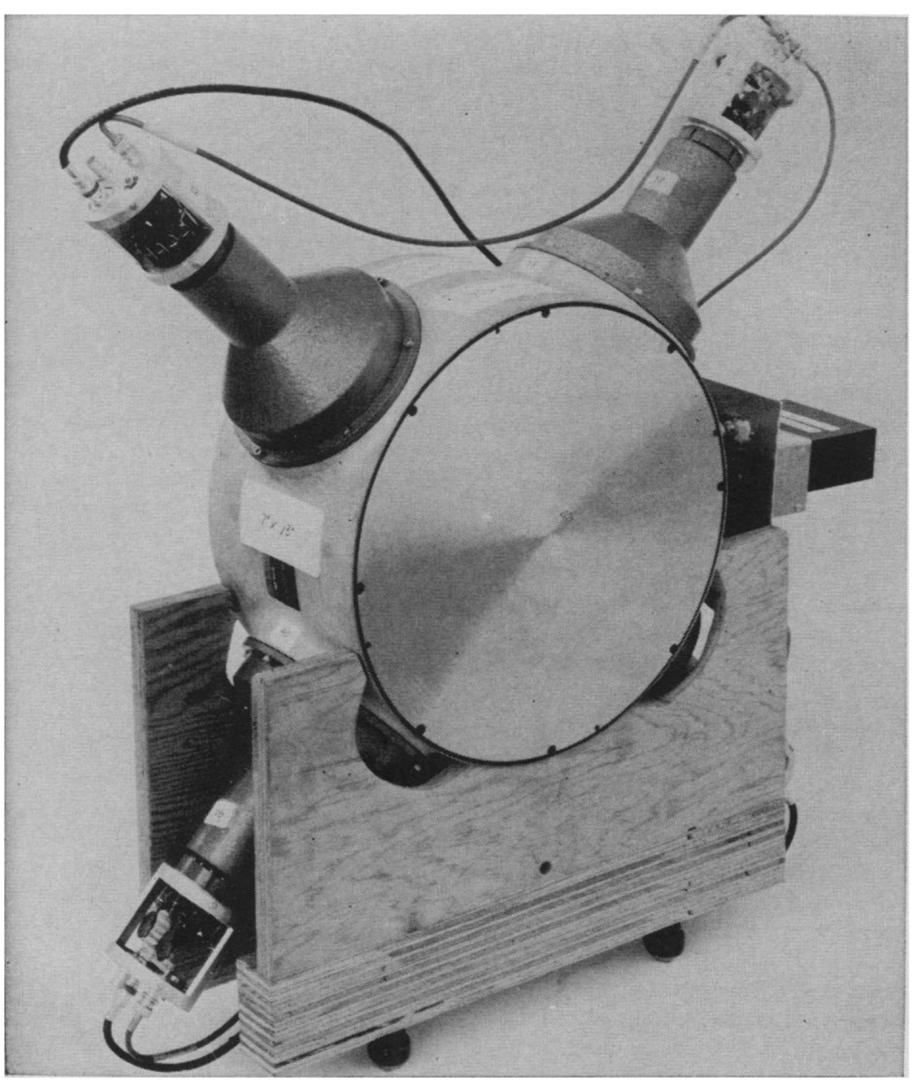

Fig. 1 (top left). Scintillation spectrum in a NaI(Tl) crystal (1 cm^3 volume) for Co^{60} radiations (*2*).

Fig. 2 (top right). Cobalt-60 gamma rays absorbed in a large crystal of NaI(Tl) (13.5 by 7 inches). The data were obtained by Hughes, Lakin, and Hofstadter (*33*).

Fig. 3 (left). The NaI(Tl) crystal and photomultipliers with which the data in Fig. 2 were obtained.

(double) Compton peak; the arrows below show the expected position of each component. When the crystal can be made sufficiently large, the Compton-scattered gamma rays are also absorbed and the Compton pulses are transferred to the total absorption peaks. Such a case is shown in Fig. 2, where the same Co^{60} radiations are captured in a large crystal of NaI(Tl), 13.5 inches in diameter and 7 inches thick. One can observe that the Compton area is greatly reduced, and the two peaks between 50 and 100 on the abscissa have become "total absorption" peaks whose combined area accounts for a large fraction of all the counts. The third peak near 160 corresponds to the capture of both the 1.17- and 1.33-Mev gamma rays at the same time: the two Co^{60} radiations are emitted simultaneously. The full width at half maximum (FWHM), which is a measure of the resolution, is approximately 6 percent for the cobalt energies. Figure 2 demonstrates that even a large crystal of the indicated size is insufficient to absorb all the radiation in the total absorption region. It must be remembered, however, that the gamma ray source (Fig. 2) was uncollimated so that some of the Co^{60} gamma rays interacted peripherally and some of the secondary Compton radiations were able to escape. Figure 3 shows a photograph of the crystal used to obtain the data in Fig. 2.

In the absorption of low-energy gamma rays the photoelectric process, the Compton process, and the pair-production processes are important. At higher energies the detection of gamma rays, electrons, and positrons depends upon the "shower" phenomenon, which in turn is derived from the bremsstrahlung and pair-production processes. A rather complete description of the electromagnetic shower process is given by Rossi (*16*). The only radiation or particles which interact significantly by showering are gamma rays, electrons, and positrons. Such radiation or particles may be called type A particles (Table 1), and detectors which depend on this process are called "total absorption shower cascade" (TASC) counters; the shower process is sketched in Fig. 4. Since the distance (one radiation length) for reproduction of the elemental shower act is about 1 inch in NaI(Tl), it may be expected that a detector whose length is 20 inches (20 radiation lengths) and whose diameter is appropriately large (say, 10 radiation lengths) can absorb the

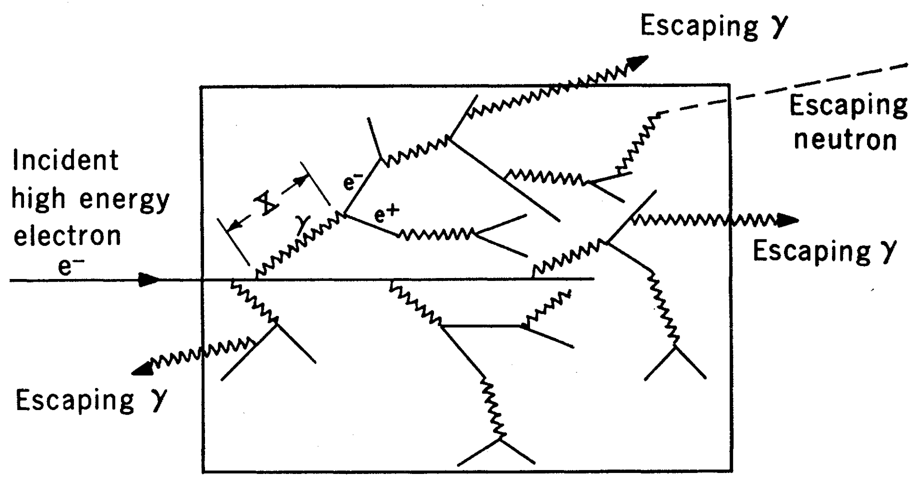

Fig. 4. The shower process. The incident particle shown is an electron. A gamma ray of high energy behaves in substantially the same way, except that the first process occurring is pair production instead of bremsstrahlung, as shown in the figure. The characteristic distance, labeled X in the figure, is approximately one "radiation length"; in NaI(Tl) this length is 1 inch.

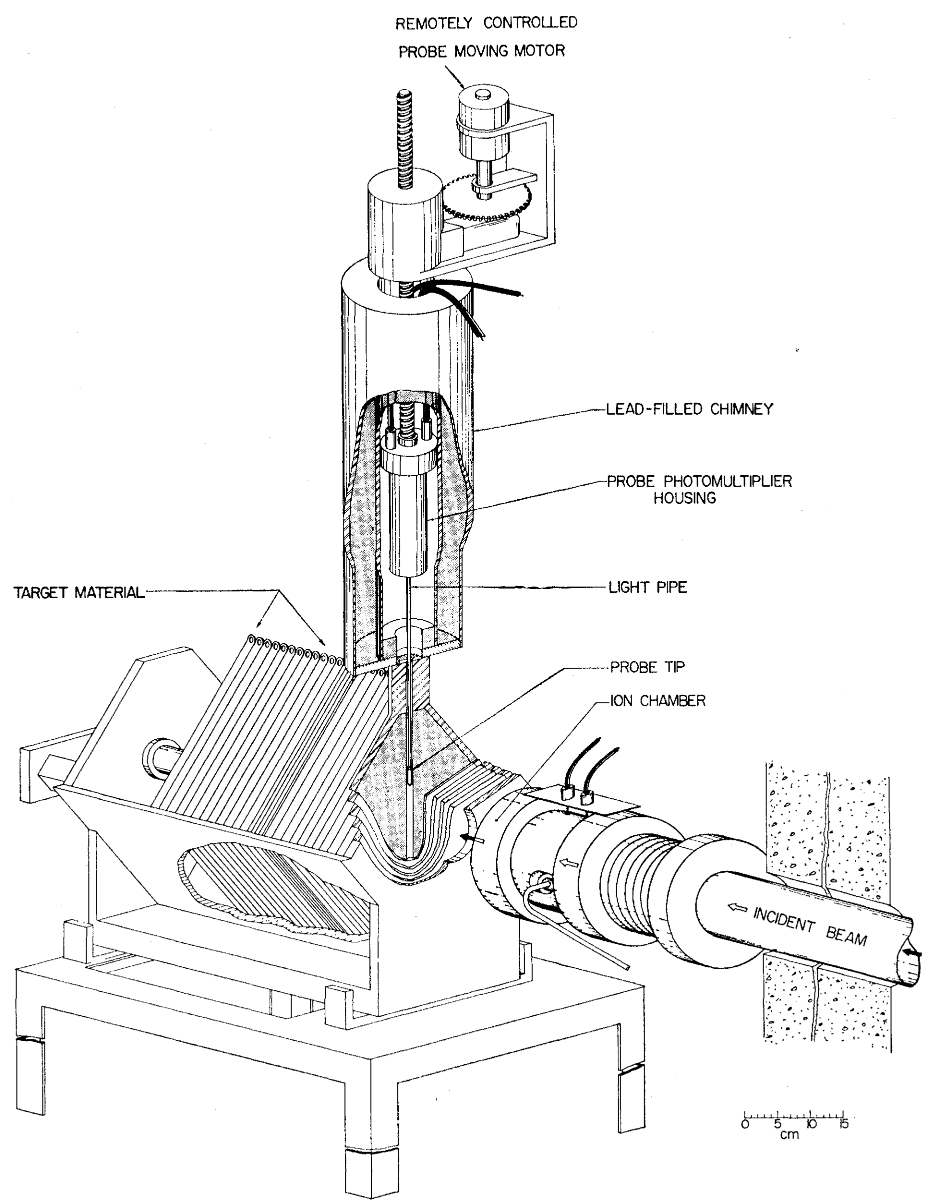

Fig. 5. Measuring apparatus of Crannell (*17*) used to trace the absorption and deposition of energy in a large metallic absorber.

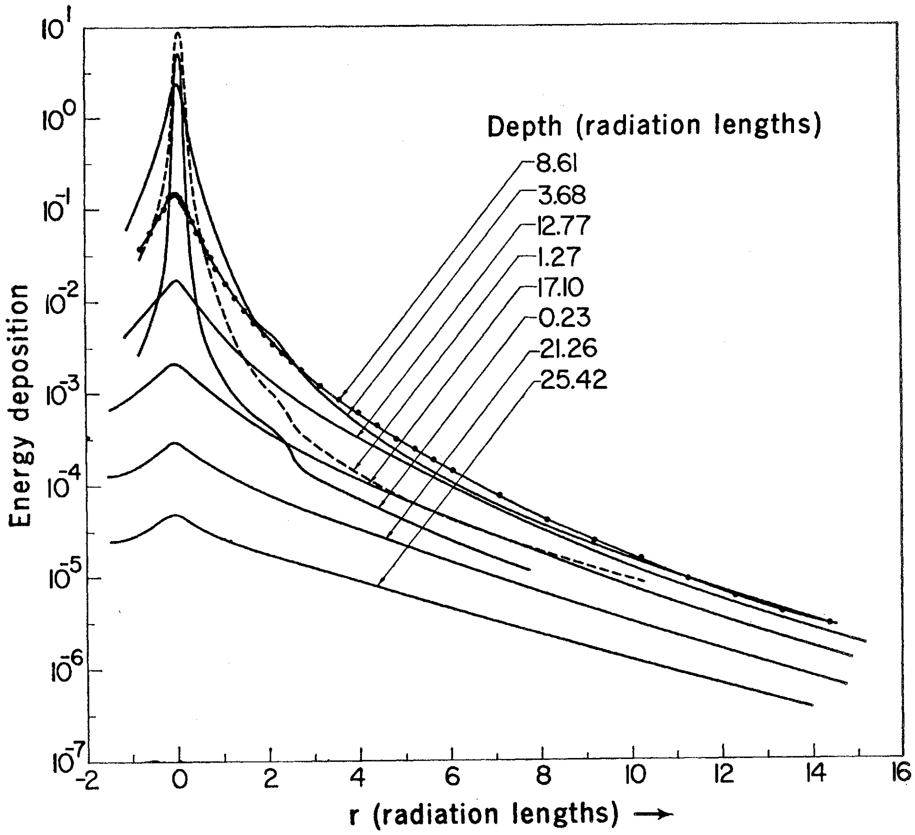

Radius in radiation lengths	0–1	1–2	2–3	3–4	4–5	5–6	6–7	7–8	8–9	9–10	10–12	12–14	14–16	16–18	18–20	20–24	24–∞
10–∞	0.01	0.02	0.03	0.04	0.04	0.04	0.04	0.04	0.04	0.04	0.07	0.07	0.06	0.05	0.04	0.04	0.05
9–10		0.01	0.01	0.02	0.02	0.02	0.02	0.02	0.02	0.02	0.04	0.03	0.02	0.02	0.01	0.01	0.01
8–9		0.01	0.02	0.02	0.03	0.03	0.03	0.03	0.03	0.03	0.05	0.04	0.03	0.02	0.02	0.02	0.01
7–8	0.02	0.01	0.02	0.03	0.04	0.04	0.04	0.05	0.05	0.04	0.08	0.06	0.05	0.03	0.02	0.02	0.02
6–7		0.02	0.03	0.05	0.06	0.06	0.07	0.07	0.07	0.07	0.12	0.10	0.07	0.05	0.03	0.03	0.02
5–6	0.02	0.03	0.05	0.07	0.09	0.11	0.11	0.12	0.12	0.11	0.19	0.14	0.10	0.06	0.04	0.03	0.02
4–5	0.02	0.05	0.08	0.12	0.15	0.18	0.19	0.20	0.19	0.17	0.29	0.21	0.14	0.09	0.05	0.04	0.02
3–4	0.04	0.08	0.14	0.22	0.28	0.33	0.35	0.35	0.34	0.29	0.47	0.31	0.20	0.12	0.06	0.05	0.02
2–3	0.07	0.16	0.30	0.47	0.61	0.70	0.71	0.68	0.62	0.50	0.76	0.47	0.27	0.15	0.07	0.07	0.02
1–2	0.15	0.48	1.11	1.74	2.06	2.10	1.90	1.55	1.31	0.98	1.31	0.70	0.35	0.17	0.08	0.05	0.01
0–1	3.62	8.54	11.4	11.4	9.68	6.92	5.17	3.49	2.41	1.55	1.70	0.72	0.30	0.13	0.05	0.03	0.01

Depth in radiation lengths

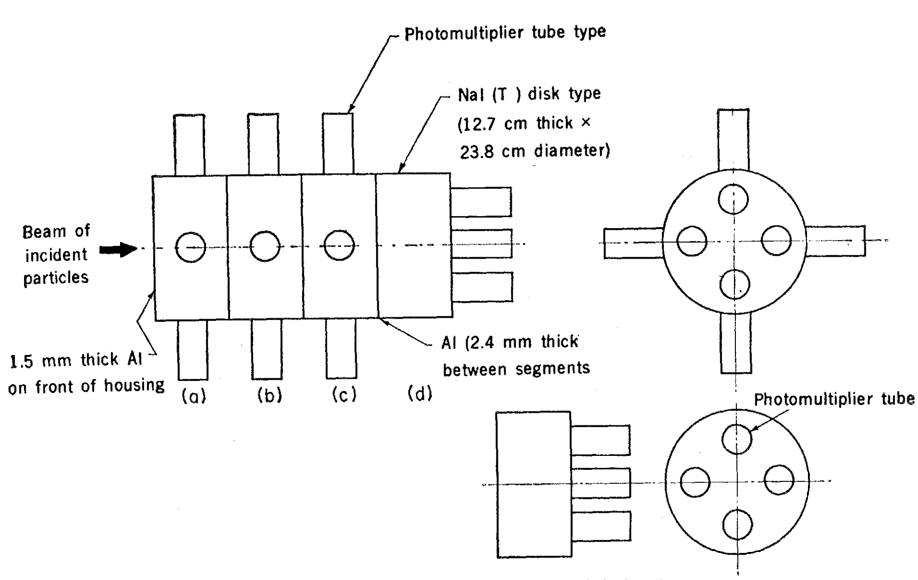

Fig. 6 (top). Radial distributions of absorbed energy of 900-Mev electrons in tin (*17*).

Fig. 7 (center). Tabulation of the relative amounts of energy (in percentage of the original energy) deposited in annular rings in the absorber. This case refers to tin at 900 Mev.

Fig. 8 (bottom). A TASC counter for type A particles which has been used successfully up to energies of 14 Bev.

whole shower. This is what is meant by total absorption.

Spreading of the shower takes place, of course, and interaction processes occurring near the surface may result in the escape of a gamma ray. In this case the absorption is not total, but the energy of the escaping, degraded gamma ray may be sufficiently low (say, 0.5 Mev for an incident energy of 1000 Mev) so that a serious loss of energy does not occur. In fact, even if a number of such gamma quanta escape, the statistics of the number of escaping packages may be large enough so that the fluctuations of escaping energy assume a Gaussian pattern. This approximate view of the escape phenomenon was taken by Kantz and Hofstadter (*1*) and provided a rough theory (*3, 4*) of the measure of resolution of energy of an incident particle or gamma ray.

The amount of energy escaping from an absorber was studied (*1*) for several elements including copper, tin, and lead. Tin was selected because its atomic number is close to that of iodide in NaI(Tl), and iodine is chiefly responsible for the absorption processes in sodium iodide scintillation crystals. Crannell (*17*) has used an apparatus of the type (*1*) shown in Fig. 5 to study how the incident energy of 900-Mev electrons is degraded and deposited throughout the interior of a large stack of tin plates. A small scintillation-type probe crystal can be moved anywhere within the stack in a radial or longitudinal position. In this way the radial curves shown in Fig. 6 are obtained (*17*). The energy is distributed through wider regions near the tail end of the absorber, whereas at the front of the absorber the curves showing the shape of the deposited energy resemble the incident beam. From such curves, the quantities tabulated in Fig. 7 can be calculated.

Figure 7 gives the relative amounts (in percentage of total energy) of energy deposited in annular rings (one radiation length in radial width) at any depth in the absorber. From such tabulations it is possible to calculate the relative amount of energy absorbed in a tin absorber of arbitrary shape. If proper allowance is made for the relative density and radiation lengths in tin and NaI(Tl), one may understand and predict the corresponding behavior of type A particle absorption at 900 Mev in NaI(Tl). The behavior at higher and lower energies has been studied experimentally (*1, 18*) and theoretically (*19*), but the main features of the shower phenomenon are not very different in the Bev range from the results at 900 Mev. One very important point emerging from these studies (*1, 4, 18, 19*) is that the depth of a TASC detector which is required to absorb, say, 95 percent of the total energy within a shower, increases only logarithmically as the energy of the incident particle is increased. Thus an increase of a factor of 10, say, from 10 Bev to 100 Bev, in the energy of an electron or gamma ray requires only an addition of about 6.0 inches in depth of new NaI(Tl) crystal material. This modest increase in detector size may be compared with the very great increases in the size of the magnetic spectrometer required to go from detection schemes at 1 Bev (*20*) to those at 8 Bev or 20 Bev (*21*). The anticipated sizes of magnetic spectrometers needed to study particles of type A having energies of 100 to 1000 Bev are too enormous to contemplate, whereas the sizes of TASC counters needed in this energy range will prove to be very modest.

Performance of TASC detectors. We now turn to a description of the present performance of TASC detectors. An early unit (*8*) is shown schematically in Fig. 8, and a photograph of a recent experimental TASC detector is shown in Fig. 9 (*22*). Figure 10 shows the sharp spectral distribution obtained with incident electrons selected magnetically at 8 Bev/c, where c is the speed of light. The behavior of positrons and gamma rays is practically identical with the pulse height distribution observed for electrons. Even better performance is obtained at 14 Bev/c (Fig. 11). The trend of the data is shown in Fig. 12 (*23*) where the resolution figure (FWHM) is plotted for two different mean diameters of TASC detectors.

The possible reasons for the observed width have been discussed by Hofstadter, Hughes, Lakin, and Sick (*22*). It is theoretically possible that greatly improved resolution can be obtained with larger crystals in which the escape of gamma rays can be minimized (*24*). Surprisingly, the FWHM at lower energies (50 Mev to 1 Bev) is on the order of 5 percent. From such data it appears that a reduction in the FWHM may require larger diameters at low energies or that a "channel" crystal at the front may be needed to stop backwardly escaping radiation. The depth of the TASC detector employed in these measurements is known to be adequate (*22*) at all energies studied thus far. The attractive small values of FWHM at high energies (~ 1 percent at 14 Bev/c) augur a most promising future for TASC detectors at still higher energies of type A particles.

The calibration of a TASC detector (*23*) is shown in Fig. 13. The observed

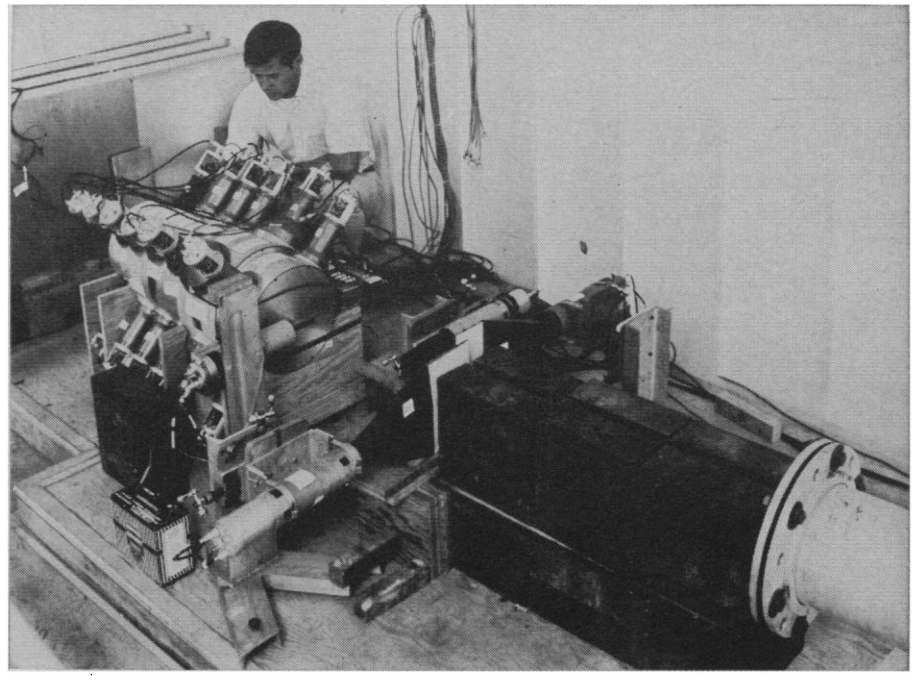

Fig. 9. A NaI(Tl) TASC detector of average diameter ≅ 11 inches and depth 28 inches. The incident beam passes through a small hole in the steel collimator to the right and impinges on the NaI(Tl) stack after passing through thin defining counters.

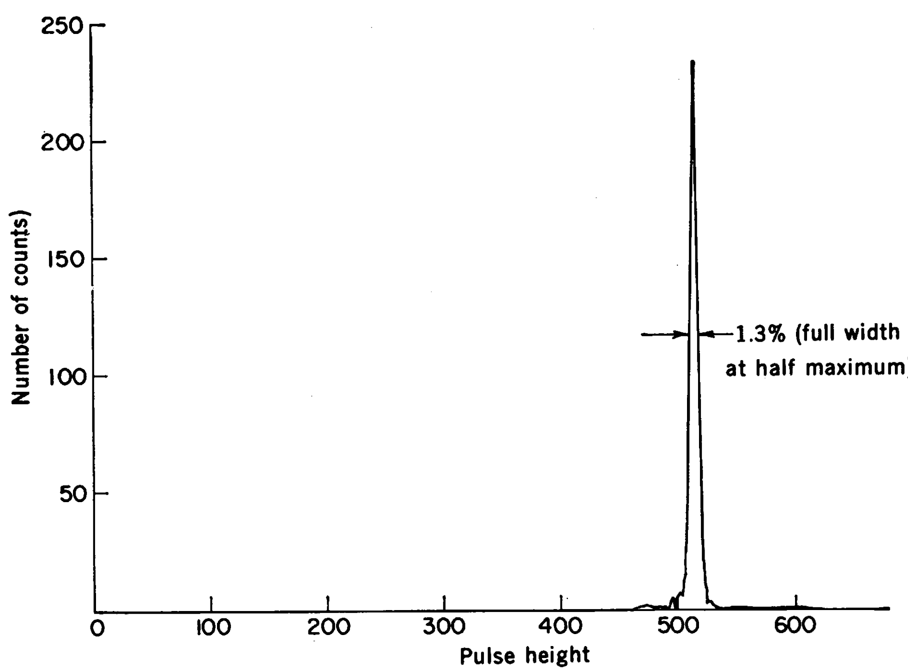

Fig. 10. The pulse height distribution (*22*) of a NaI(Tl) (20 inches in length and 9.37 inches in diameter) TASC detector for 8 Bev/c electrons.

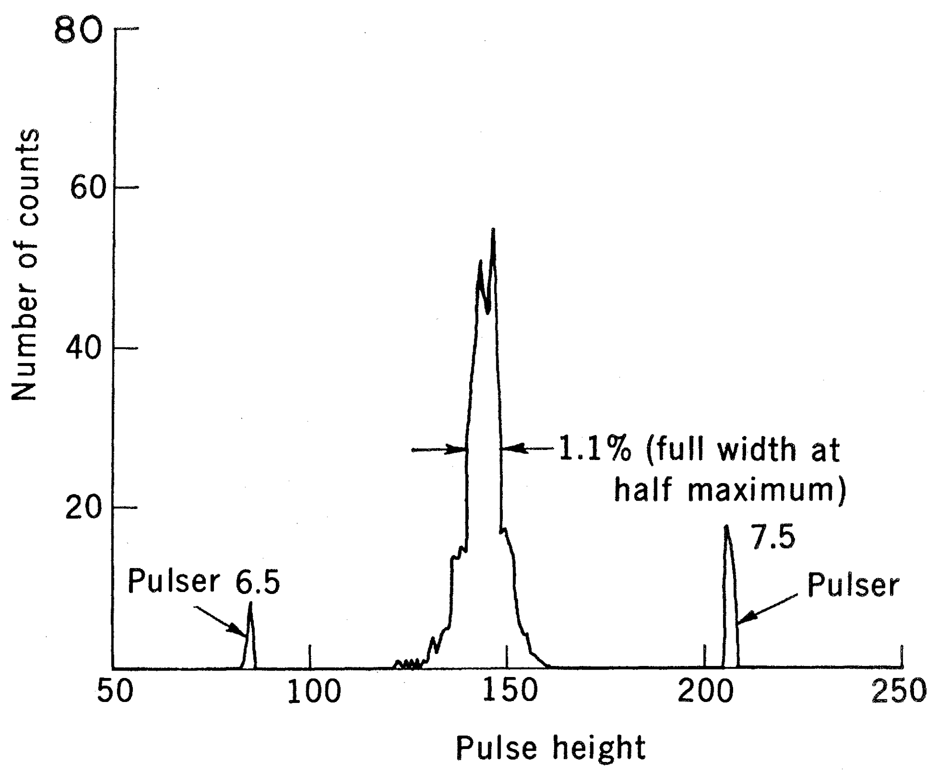

Fig. 11. The pulse height distribution (*22*) of a NaI(Tl) (20 inches in length and 9.37 inches in diameter) TASC detector for 14 Bev/*c* electrons. Note the artificial pulser calibration and the suppressed zero.

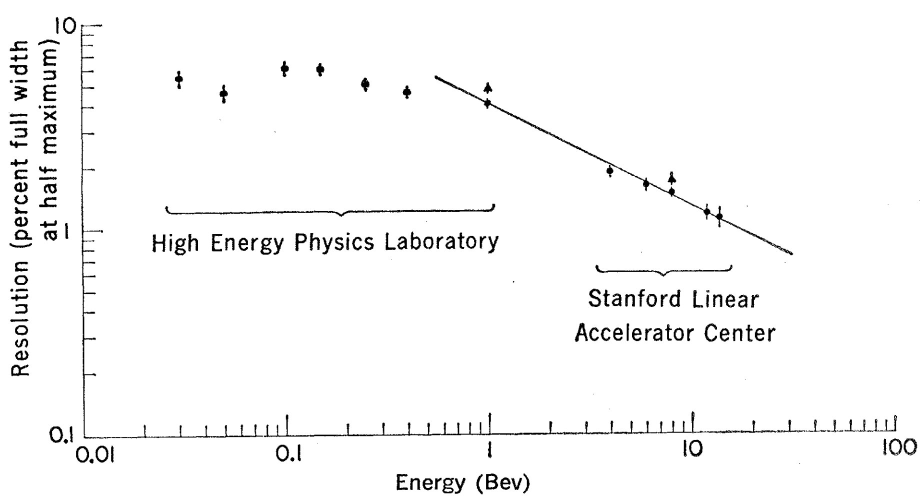

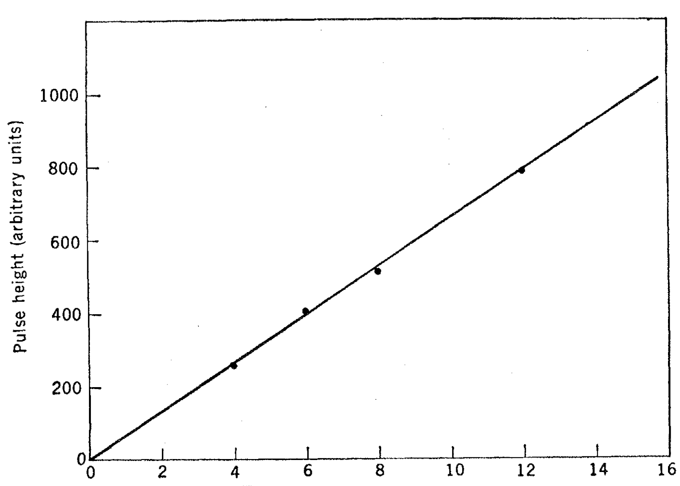

Fig. 12 (above left). The resolution figure (FWHM) plotted as a function of energy. Results are shown for a NaI(Tl) crystal 11.5 inches in diameter and 23 inches in length (●) and for a NaI(Tl) crystal, 9.37 inches in diameter and 20 inches in length (▲).

Fig. 13 (left). Pulse height of the peak plotted against electron energy for a NaI(Tl) TASC detector.

behavior is linear as is the case for all TASC detectors for which experiments have been carried out thus far (*8, 22, 23*).

The performance of TASC detectors does not deteriorate until the beam is allowed to approach the periphery of the crystals. This behavior (*23*) (Fig. 14) indicates that adequately large solid angles are assured for detection of type A particles by TASC detectors.

The performance of a NaI(Tl) TASC detector that directly faces a liquid-hydrogen target in an actual experimental arrangement at the Mark III linear accelerator of the Stanford High Energy Physics Laboratory is shown in Figs. 15, 16, and 17 (*25*). These results are very impressive because of the extremely high radiation backgrounds present in the target areas of linear electron accelerators. The backgrounds are due basically to the high beam currents and the short duty periods of such accelerators. Figure 15 shows the spectrum of electrons and gamma rays scattered at an angle of 110° from a liquid-hydrogen target for an incident beam of 1×10^{10} electrons per pulse at an incident energy of 200 Mev. At the right one observes an elastically scattered peak of electrons. The continuum at the left consists mostly of gamma rays. Figure 16 shows the electron spectrum without the gamma rays; the gamma rays have been eliminated by use of a gate obtained from a coincidence telescope of plastic scintillation counters placed in front of the TASC detector. When the incident energy is increased to 400 Mev (Fig. 17), a pion distribution is also observed, as indicated (at position 27) by the large peak to the left of the elastically scattered electron peak near position 72. This case provides an example in which

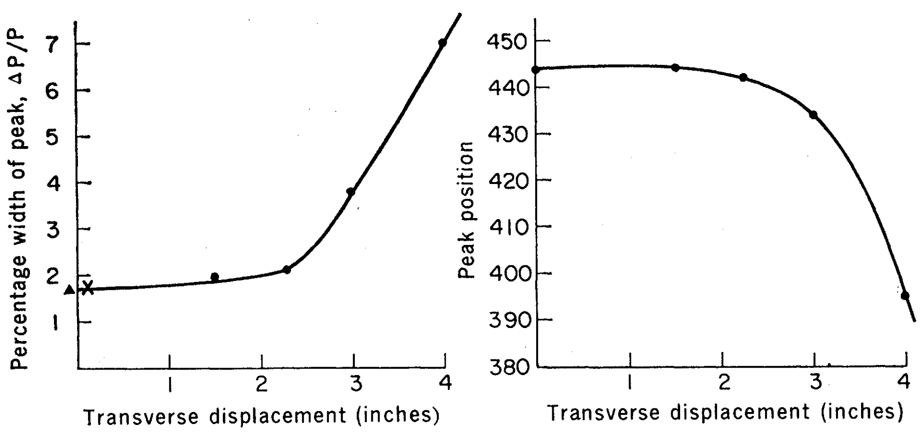

Fig. 14. Behavior of a NaI(Tl) TASC detector as a function of the position of entrance of the beam of incident particles. The resolution is shown at left and peak height to right. The outside radius of the crystal was approximately 4.6 inches.

pions may be distinguished from electrons. These results were obtained (*25*) when the TASC detector was enclosed in a concrete shielding "cave" mounted on a movable carriage. The weight of the cave was about 60 tons, which is more than adequate to shield against the observed background. It is not anticipated that larger or more massive shields are needed at higher energies. Moreover, with continuous-duty machines such as superconducting linear accelerators, or with electron or proton synchrotrons, it is likely that only very thin shields, if any, will be required.

TANC detectors for "strongly interacting" or Type B particles. The problem of the detection and measurement of strongly interacting type B particles at very high energies represents a formidable challenge to present technical skills. One possible approach is provided by the use of "total absorption nuclear cascade" (TANC) detectors (*9*). For such detectors it is immaterial whether the particle is charged or uncharged since the initial detection event depends only on the strong interaction process. In this process a struck nucleus is broken up so that the particles released by it, both charged and uncharged, are the actual particles detected. The nuclear cascade process, upon which this method depends, was originally described by Serber (*26*). Figure 18 provides a schematic diagram of the detection process. In any nuclear explosion mesons as well as nucleons are released, and at very high energies (1000 Bev) it has been estimated that 85 percent of the energy is released in the form of π° mesons (*12*, p. 262). This is very favorable for detection since the neutral pions decay immediately into gamma rays which are readily detectable by TASC counters. Thus if we use the total absorption method and if the detector is large enough, a very large fraction of all the energy of the incident particle can be absorbed and measured. This principle has been discussed at length, and other advantages of TANC counters have been described (*9*). When the detector is appropriately large, the energy resolution (FWHM) will be limited only by residual escape of neutrons, fluctuations in the energy absorbed in the nuclei because of the binding energy of the nucleons, and the number of

Fig. 15 (left). Results obtained on a multichannel analyzer with a TASC counter 15 inches long exposed to the radiation emitted by a liquid-hydrogen target struck by 200-Mev electrons. The peak at the right corresponds to elastically scattered electrons. The continuum at the left corresponds to gamma rays. The number of electrons per pulse was 1×10^{10} and the scattering angle was 110°.

Fig. 16 (below). The data obtained here are similar to those in Fig. 15 except that the gamma ray continuum, to the left in Fig. 15, has been eliminated by a coincidence telescope.

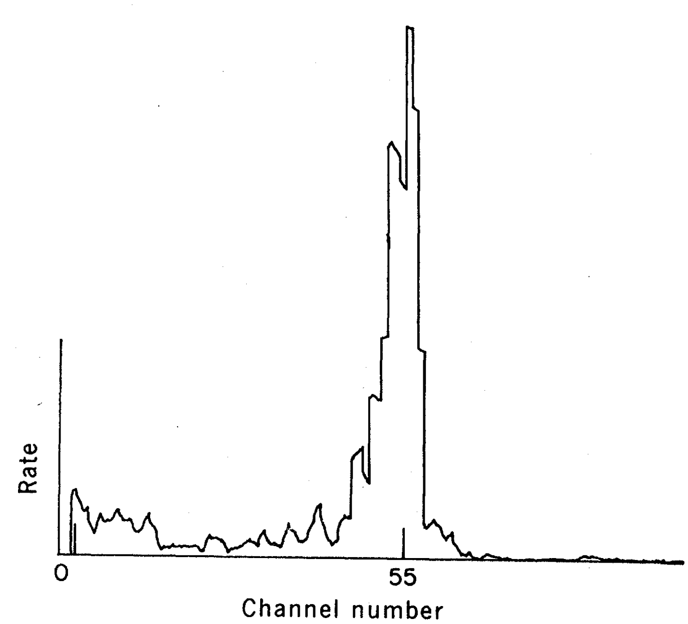

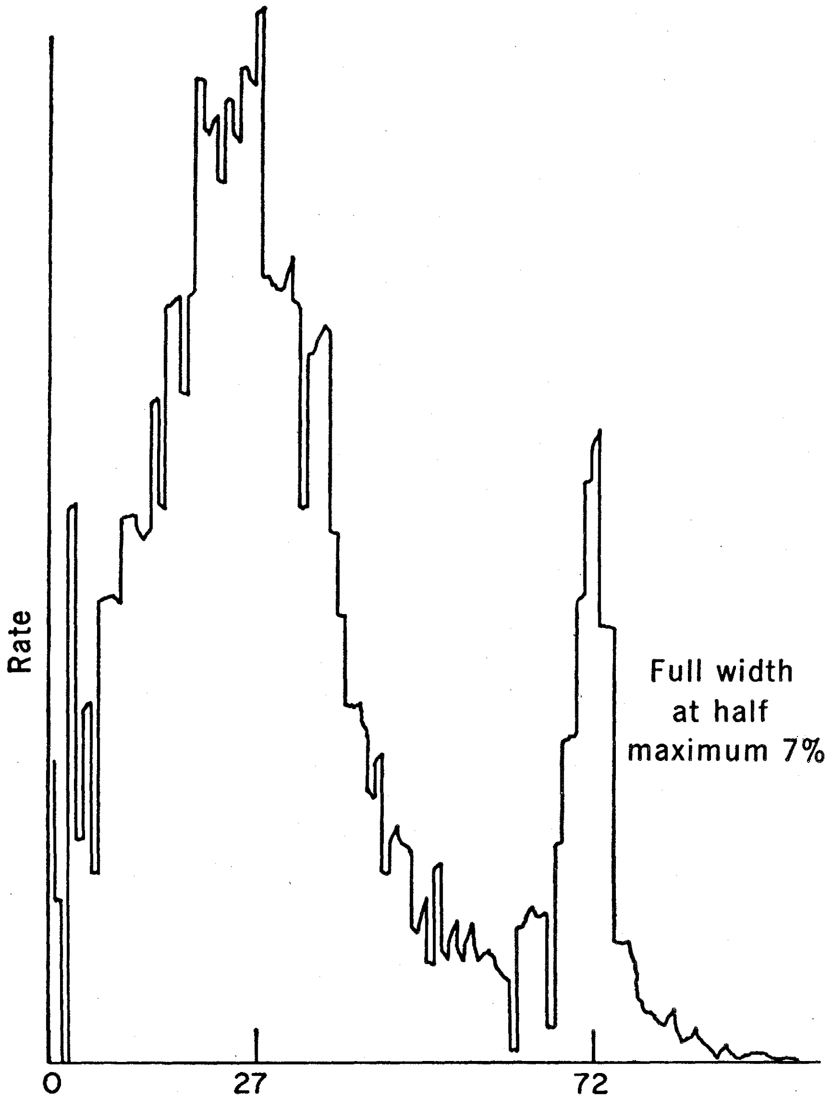

Fig. 17. The data are similar to those in Fig. 16 except that the incident energy has been increased to 400 Mev. The peak at the left consists almost entirely of pions.

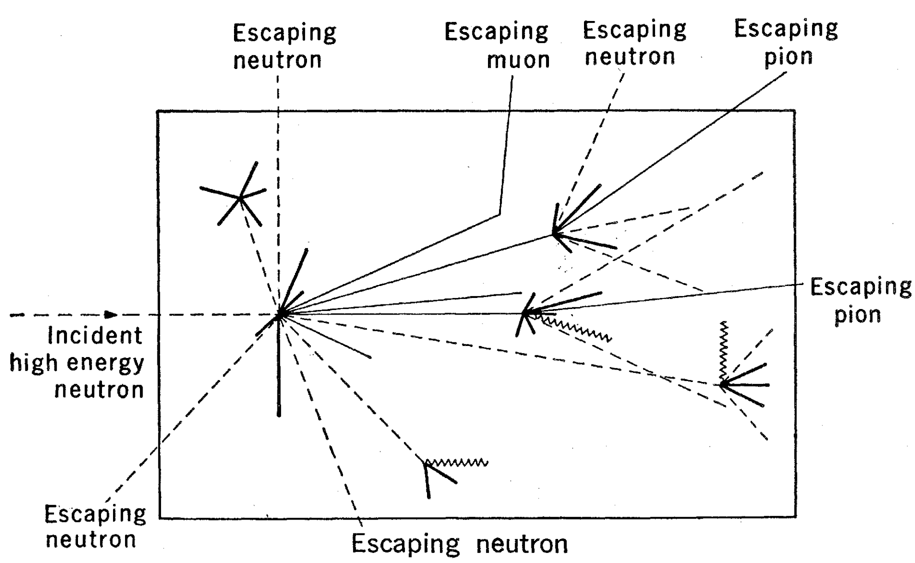

Fig. 18. Schematic view of the detection process for a TANC detector. Some neutrons and pions can escape from the detector. In the nuclear collisions some binding energy is lost that may not be recovered in the crystal during the event. Positive pions may also decay and some of their end products may be lost from the detection process.

positively charged pions or kaons, and so forth, which stop and decay in the detector. The latter subsequently give rise to neutrinos and the relatively long-lived muons during their decay.

Pions and nucleons are often emitted from struck nuclei at large angles with respect to the direction of the incident high-energy particle. Thus the proposed TANC detector should have large lateral dimensions. Furthermore, the absorption length for high-energy, strongly interacting type B particles is of the order of 15 inches in NaI(Tl), as contrasted with the corresponding value of 1 inch for type A particles. In order to absorb all the incident energy, the TANC detector must be larger than a TASC detector. How large should a TANC detector be to yield good resolution? A preliminary answer to this question is provided by studies made of the deposition of energy of 8 Bev/*c* pions in absorbing materials (*27*). These studies were made by a method completely analogous to that described by Kantz and Hofstadter (*1*) and by Crannell (*17*). The results obtained for a stack of tin plates are shown in Fig. 19. The curves indicate the amount of energy deposited at various radii at different longitudinal depths in the absorber and are analogous to those of Fig. 6. From the curves of Fig. 19, one can prepare a table for pions similar to that shown in Fig. 7 for electrons. From such measurements and calculations one can obtain the "containment" of energy in a given absorber struck by 8 Bev/*c* pions.

Figure 20 shows the relative percentage of the energy of the incident pion contained in a tin absorber of very great longitudinal depth whose cylindrical radius is given on the abscissa; "very great" depth in this instance means about 40 inches of tin (*28*). The measured curve (energy deposited) shows that for a radius of 0.38 absorption length, approximately 52 percent of the energy is absorbed on the average. The diameter of an equivalent absorber of NaI(Tl) used in the tests is approximately 11.2 inches. When a correction (*28*) is made for the 56.0-inch length of the actual experimental NaI(Tl) TANC assembly, the relative absorbed energy is in the neighborhood of 45 percent. Experiments have been carried out with this TANC detector and 8.0 Bev/*c* incident pions. The results are shown in Fig. 21.

Three "peaks" are evident in the figure. The sharp peak at the right is a calibration peak obtained with type A particles—electrons in this case. The very broad peak in the middle corresponds to the nuclear interaction events induced by the 8 Bev/c pions. The peak at the left corresponds partly to those pions ($\sim$ 2 percent in number) which have engaged only in Bethe-Bloch collision-loss processes in the stack of crystals. Such pions give rise to the well-known Landau straggling distribution. A larger part of this peak corresponds to a muon contamination in the pion beam.

From the average pulse height in the nuclear interaction peak, one may note the approximate agreement between the average fraction of 49 percent of the total energy absorbed experimentally in the nuclear interaction peak and the calculated figure of 45 percent obtained from the measurements in the tin absorber. It is also most important to observe that there are some pion interaction pulses lying near channel 200 which have essentially the whole energy of the incident pions. Thus the TANC method of detection of strongly interacting particles would seem to be justified in principle.

The broad distribution of pulses in the nuclear interaction peak shows also that there is a large, variable amount of energy escaping from the crystal. It has been shown experimentally (*27*) that the escaping energy goes out mostly in the form of neutrons, though there may be a small amount of energy escaping in charged particles. Neutrons in the energy range from 10 to 50 Mev are the particles most likely to escape.

The observed width (FWHM) of the middle peak is about 65 percent. It is difficult to compare this with even a rough theory since the amount of escaping energy is itself on the order of 55 percent. The type of crude theory used for escaping gamma rays in TASC counters can probably be employed in this case only when a larger fraction of the incident energy is absorbed. Nevertheless, it is to be expected that, as the radial dimensions of the TANC counter are increased, the nuclear interaction peak will move up toward the calibration peak position and will become much narrower.

Preliminary data (*27*) show that, when the average radius of the crystals is increased from 9.2 inches to 11.2 inches, the average pulse height of the nuclear interaction pulses moves from a value of 40 percent for the average amount of energy absorbed to a corresponding figure of 45 percent. This is very promising for the proposed

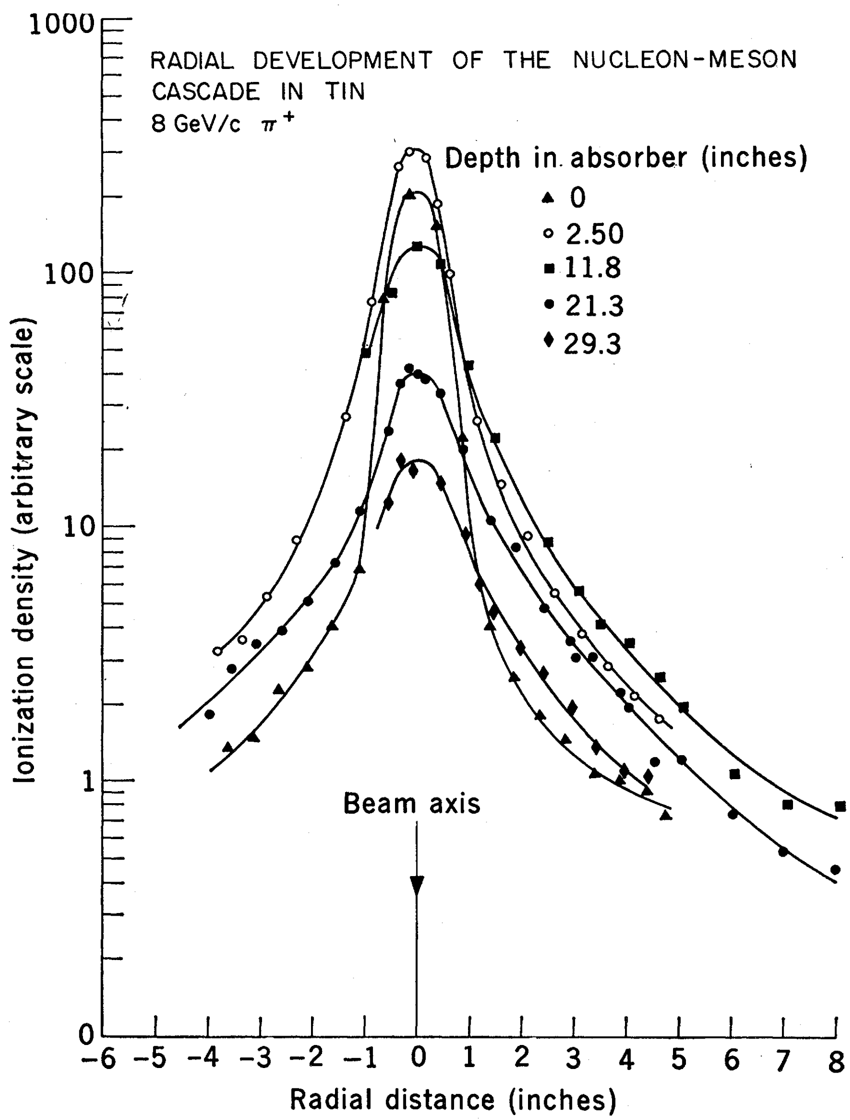

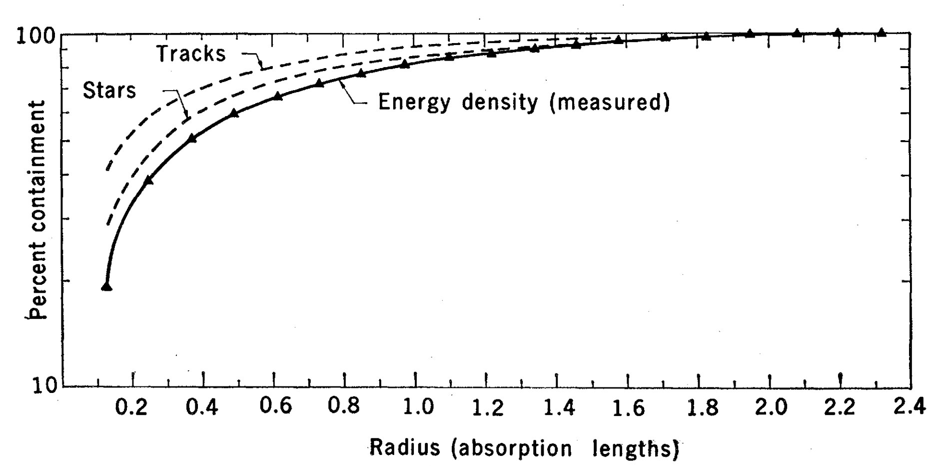

Fig. 19 (top right). Radial spread in the development of nucleon-meson cascades in tin produced by 8 Bev/c positive pions.

Fig. 20 (right). Containment curve of energy deposited in tin by 8 Bev/c pions. The solid curve is measured whereas the star and track data are obtained from Monte Carlo calculations (*32*).

TANC detection technique and is in accord with the results in Fig. 20. Preliminary data (*27*) further indicate that, for pions in the energy range from 4 Bev/*c* to 16 Bev/*c*, the observed maximum of the nuclear interaction peak is directly proportional to the energy of the incident pions. From work in progress it is expected that experimental measurements will be made with NaI(Tl) crystals 16 inches in diameter and subsequently with others 30 inches in diameter. In the latter case it may be possible to achieve resolution figures (FWHM) lying somewhere between 2 and 12 percent.

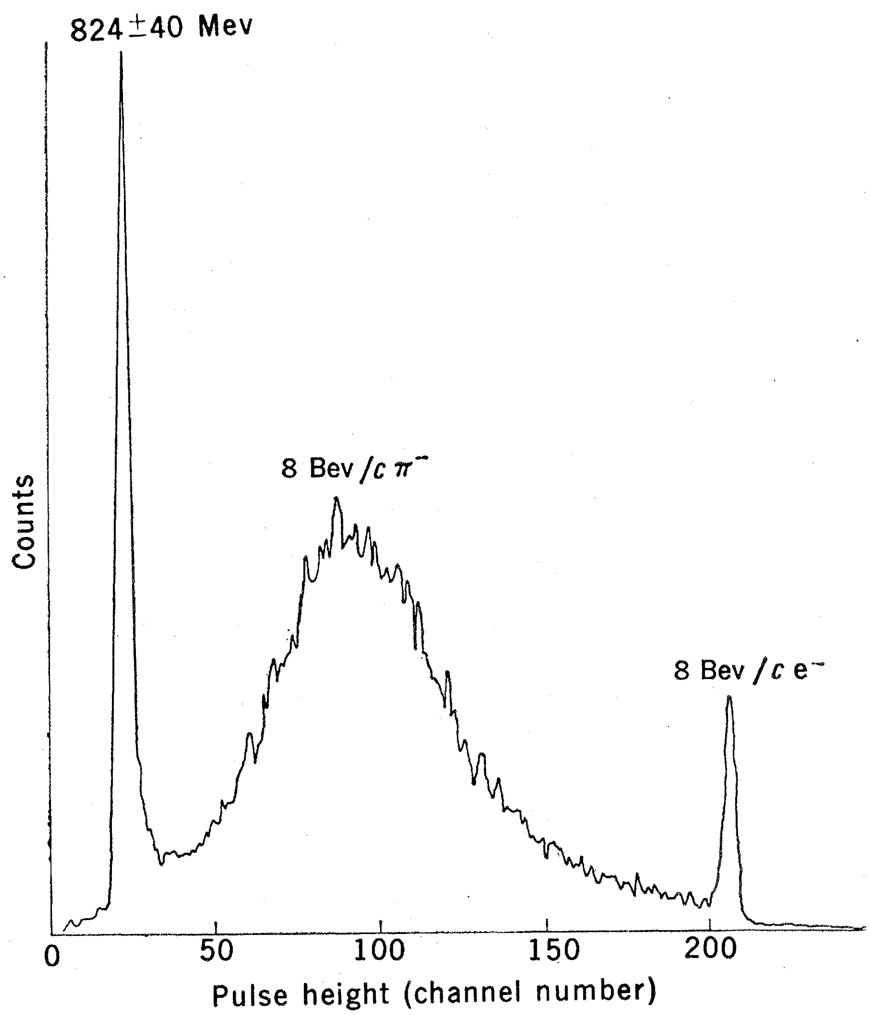

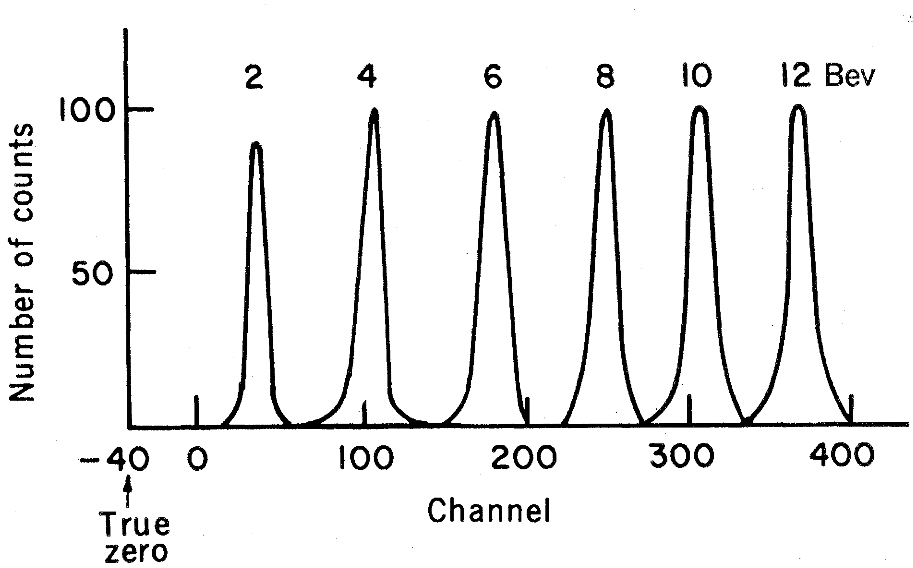

Outlook for the Future

It has already been pointed out (*9*) that total absorption detectors may be made in various ways as (i) scintillation counters; (ii) Cerenkov counters; and (iii) semiconductor or crystal conductor-type counters. Also liquid or glassy materials may be used if their densities are high enough. Some results of recent work with PbF_2 Cerenkov detectors for type A particles are shown in Fig. 22 (*7*). The PbF_2 detector used here is small enough to be held in one hand! Although the resolution achieved corresponds at the highest energy to a FWHM of 5 percent, theory (*7*) indicates that this figure can probably be reduced still further. If PbF_2 material could be made into a scintillation counter material, this achievement could result in a fantastic reduction in the size of equipment need for work in high- and super-high-energy physics.

In all probability luminescent or conduction processes are not the only ones amenable to total absorption methods of detecting high-energy radiation. It may be that heat-detecting (infrared) or sound-detecting devices may also be employed. In the latter case it is possible that the most dense materials, such as tungsten, could be used as the absorbing substance, and resonant acoustic vibrations of the absorbing block could be measured with equipment tuned to the resonant frequencies of the absorbing body. Piezoelectric or ferroelectric materials, for example, could be used to detect these vibrations. A piezoelectric material may itself be used as the absorber material.

In any case, it is possible that as physicists proceed with the detection of higher and higher energies possessed by single particles, the detection techniques may become easier instead of more difficult! This would indeed be a major contribution of the total absorption technique.

One may also take advantage of the energy-detecting ability of total absorp-

Fig. 21 (top left). Pulse height distribution of 8 Bev/*c* pions in a TANC NaI(Tl) 56 inches long and about 11.2 inches in mean diameter.

Fig. 22 (left). Pulse height distributions of 2- to 12-Bev electrons in a small PbF_2 (5.25 by 5 inches) Cerenkov detector (*7*). The crystal was viewed by a single photomultiplier.

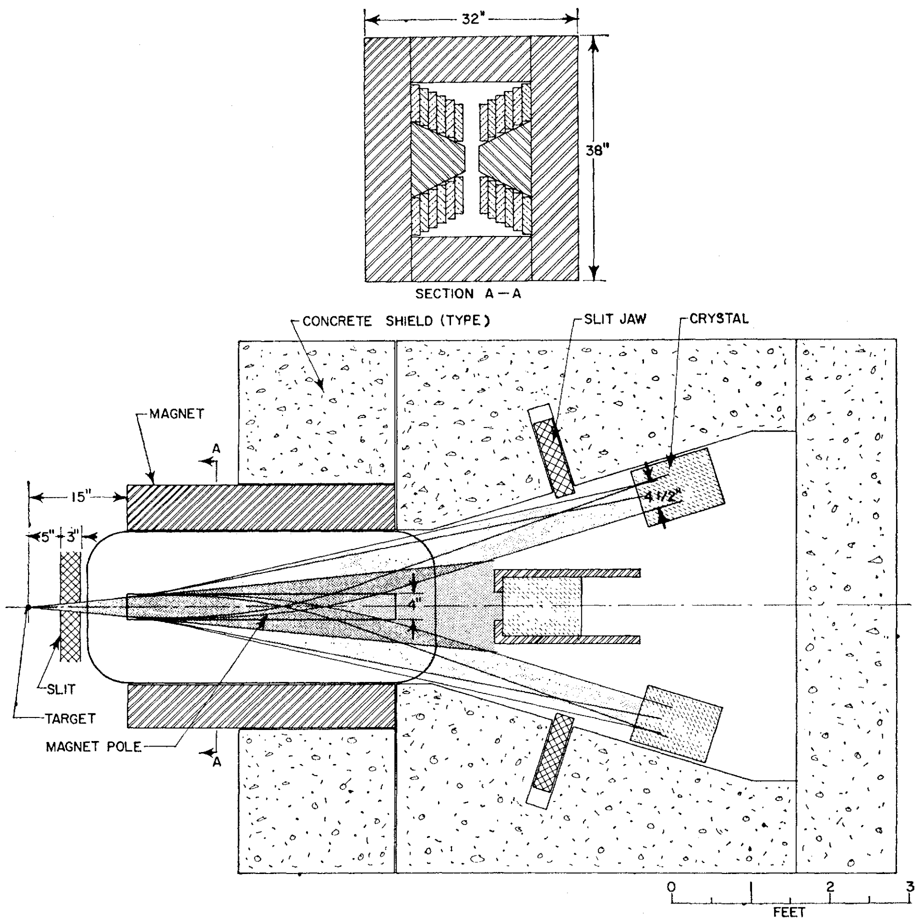

Fig. 23. Schematic diagram showing how magnetic means can be combined with TASC or TANC detectors to obtain, simultaneously, energy data on positively and negatively charged particles and gamma rays (*29*). The crystal detector system diagrammed here has the following specifications: 2-Bev maximum energy; 30 percent momentum range accepted by spectrometer ($\Delta P/P$); 0.01 solid angle acceptance range of spectrometer (200 by 50 milliradians); 24 kilogauss; gap 2 inches; magnet weight 7 tons; magnet power 57 kilowatts.

tion counters by combining these counters with simple magnetic means. Figure 23 shows a proposed scheme (*29*) for the construction of a relatively small unit for the simultaneous detection of positively charged particles, negatively charged particles, and gamma rays. The optics of the magnetic spectrometer need only be primitive since the energy determination is made by the crystal means. The system pictured has a wide dynamic range (30 percent), large solid angle, and an energy resolution determined solely by crystal performance.

One can think of many experiments in elementary particle physics that can be carried out with the total absorption techniques described in this paper. As a example, a NaI(Tl) detector was used in a recent experiment in which K_L° total cross sections were measured in various elements (*30*). The neutral kaons had energies in the range from 6 to 12 Bev/*c*. Such cross sections can be compared with neutron total cross sections at 27 Bev/*c* measured by the Brookhaven-Michigan collaboration group (*31*). Differences have been observed between the neutron and K_L° cross sections, and such differences may provide the basis of a new method for the studying of nuclear radii.

Conclusion

Although the results reported in this paper represent only the beginnings of what may develop into a much more sophisticated field of detectors, it is possible at this time to compare the TASC and TANC detectors with what might be considered the "perfect" detector. A perfect detector might have the following characteristics: (i) 100 percent detection efficiency; (ii) high-speed counting and timing ability; (iii) good energy resolution; (iv) linearity of response; (v) application to virtually all types of particles and radiations; (vi) large dynamic range; (vii) virtually no limit to the highest energy detectable; (viii) reasonably large solid angles of acceptance; (ix) discrimination between types of particles; (x) directional information; (xi) low background; and (xii) picturization of the event.

Some of these characteristics have been touched on in the text. Some have been discussed by Hofstadter (*9*). In any case it is clear that TASC and TANC counters are endowed with many of the desirable qualities listed above. For example, with reference to item (xii), the possibilities inherent in the "luminescent chamber" may someday be applied to TASC and TANC counters. With respect to item (x), hodoscopes may easily be used in conjunction with the counters. Combinations of different materials may be used to fabricate TASC or TANC counters to make possible the realization of item (ix). With all these possibilities available, the picture looks bright for further development of total absorption techniques.

References and Notes

1. A. Kantz and R. Hofstadter, *Phys. Rev.* **89**, 607–617 (1953) (in particular, p. 617); *Nucleonics* **12**, 36 (1954).
2. J. A. McIntyre and R. Hofstadter, *Phys. Rev.* **80**, 131 (1950).
3. A. W. Knudsen and R. Hofstadter, *Trans. IRE (Inst. Radio Eng.) Nucl. Sci.* **NS-5**, 152 (1958).
4. R. Hofstadter, in *Methods of Experimental Physics in Nuclear Physics*, L. C. L. Yuan and C. S. Wu, Eds. (Academic Press, New York, 1961), vol. VA, p. 652.
5. S. Berezin, R. Hofstadter, M. R. Yearian, *Bull. Amer. Phys. Soc.* **7**, 620 (1962); S. Berezin, thesis, Stanford University (1966).
6. E. Dally and R. Hofstadter, *Rev. Sci. Instrum.* **39**, 658 (1968).
7. ———, *IEEE (Inst. Elec. Electron Eng.) Nucl. Sci.* **NS-15** (3), 76 (June 1968).
8. W. L. Lakin, E. B. Hughes, R. Hofstadter, *ibid.*, pp. 82–83.
9. R. Hofstadter, *Nucl. Instrum. Methods* **63**, 136 (1968).
10. R. Hofstadter, in *Meson Spectroscopy*, C. Baltay and A. H. Rosenfeld, Eds. (Benjamin, New York, 1968), pp. 443–454.
11. N. L. Grigorov, V. S. Murzin, I. D. Rapaport, *J. Exp. Theor. Phys.* **7**, 348 (1958).
12. V. S. Murzin, *Progr. Elem. Particle Cosmic Ray Phys.* **9**, 247 (1967).
13. P. V. Ramana Murthy, B. V. Sreekantan, A. Subramanian, D. Verma, *Nucl. Instrum. Methods* **23**, 245 (1963).
14. C. A. Heusch, in *Proceedings of the International Symposium on High-Energy Electrons, 1964*, G. Höhler, G. Kramer, U. Meyer-Berkhout, Eds. (Springer-Verlag, Berlin, 1966), vol. 2, p. 408.
15. Although the detectors discussed in this paper may develop into very good detectors for type C particles, we will not present any elaboration of this technique in this review.
16. B. B. Rossi, *High Energy Particles* (Prentice-Hall, Englewood Cliffs, N.J., 1956).
17. C. Crannell, *Phys. Rev.* **161**, 310 (1967).
18. G. Bathow, E. Freytag, K. Tesch, *Nucl. Phys.* **B2**, 669 (1967); Y. Murata, *J. Phys. Soc. Jap.* **20**, 209 (1965).
19. H. Nagel, *Z. Phys.* **186**, 319 (1965); C. D. Zerby and H. S. Moran, *J. Appl. Phys.* **34**, 2445 (1963); U. Völkel, *Deutsches Elektronen Synchrotron Rep. No. 65/6* (1965) (Hamburg, Germany).

20. R. Hofstadter, F. Bumiller, B. R. Chambers, M. Crossiaux, *Proceedings of the International Conference on Instrumentation for High-Energy Physics* (Interscience, New York, 1960), pp. 310–315.
21. W. K. H. Panofsky, *Springer Tracts Mod. Phys.* **39**, 138 (1965).
22. R. Hofstadter, E. B. Hughes, W. L. Lakin, I. Sick, *Nature* **221**, 228 (1969).
23. ———, in preparation.
24. When the statistics of photoelectrons at the photomultiplier surface are considered, 0.02 percent is the limiting resolution at 10 Bev.
25. B. L. Beron, R. Hofstadter, E. B. Hughes, W. L. Lakin, I. Sick, in preparation.
26. R. Serber, *Phys. Rev.* **72**, 1114 (1947).
27. E. B. Hughes, W. L. Lakin, I. Sick, R. Hofstadter, *High Energy Phys. Lab. Rep. No. 592*, in preparation.
28. A "transition" curve showing energy absorbed plotted against longitudinal depth has also been obtained and is used in making the necessary correction for finite depth of absorber.
29. W. Wadensweiler, B. Chambers, E. E. Chambers, R. Hofstadter, personal communication.
30. W. L. Lakin, R. Hofstadter, E. B. Hughes, L. Madansky, paper presented at the Washington meeting of the American Physical Society, April 1969 (*High Energy Phys. Lab. Rep. No. 600*).
31. M. M. Kreisler, L. W. Jones, M. J. Longo, J. R. O'Fallon, *Phys. Rev. Lett.* **20**, 468 (1968).
32. J. A. Geibel and J. Ranft, *Nucl. Instrum. Methods* **32**, 65 (1965); J. Ranft, *Cons. Europe. Rech. Nucl. Rep. MU/EP 66-8* (1966).
33. E. B. Hughes, W. L. Lakin, R. Hofstadter, unpublished results.
34. I thank the following individuals for their kind help in providing many of the results reported in this paper: B. L. Beron, E. B. Dally, E. B. Hughes, W. L. Lakin, L. Madansky, J. J. Murray, L. O'Neill, and I. Sick. In particular, I wish to thank Dr. E. B. Hughes for numerous and profitable discussions. I would also like to acknowledge the support of a gift grant made available by the General Motors Corporation. Work supported in part by the U.S. Office of Naval Research under contract Nonr 225(67).

CURRENT PROBLEMS IN RESEARCH

Polywater

Vibrational spectra indicate unique stable polymeric structure.

Ellis R. Lippincott, Robert R. Stromberg, Warren H. Grant, Gerald L. Cessac

A form of water with properties very different from those well established for water has been reported in a series of papers by Deryagin and coworkers (*1*). Water in this unusual state has been called "anomalous water" by this group to distinguish it from ordinary water. It has been prepared in two ways. As described by Fedyakin (*2*), secondary columns were observed growing near both ends of a column of water sealed in a glass capillary 2 to 4 μm in diameter. In subsequent work, the anomalous water was prepared by the condensation of water vapor in glass and fused quartz capillaries at relative pressures somewhat less than unity (*3*). Some of the reported properties of this water are (i) low vapor pressure; (ii) solidification at $-40°C$ or lower temperatures to a glass-like state with a substantially lower expansion than that of ordinary water when it freezes; and (iii) a density of 1.01 to 1.4 g/cm^3 and stability to temperatures of the order of 500°C.

Some of the properties of this anomalous water reported by Deryagin and co-workers have been corroborated by Willis, Rennie, Smart, and Pethica (*4*). This group also investigated the infrared spectra of the material in a barium fluoride cell. They reported that they were able to obtain only a poor spectrum, that they were required to use a 5× scale expansion, and that they obtained only absorption bands characteristic of normal water.

Bellamy, Osborn, Lippincott, and Bandy (*5*) also confirmed some of the reported properties of anomalous water. They reported spectroscopic data, in the near infrared region, of distilled samples which they believe consisted of a mixture with normal water. In addition, a Raman spectrum on this material was recorded above 3000 cm^{-1}. Structures consistent with the spectra were discussed.

In all cases, the quantities of material prepared have been extremely minute because the capillaries used for its preparation are of the order of 5 to 100 μm in diameter. This has been a severe limitation in the investigation of the properties of the material and in the analyses of possible contaminants which might account for the remarkable properties. Most of the reported investigations up to now have been carried out in the capillary tubes used for the preparation.

We now report the results of an infrared and Raman spectroscopic study of this "anomalous" water both in and out of the capillaries in which it had been formed. From an interpretation of these spectra we propose that the material is a true high polymer, consisting of H_2O monomer units. The properties, therefore, are no longer anomalous but rather, those of a newly found substance—polymeric water or polywater.

The polywater used was prepared by the condensation of water vapor in freshly drawn, fused quartz and Pyrex capillaries between 5 and 20 μm in diameter. The tubing used to form the capillaries was cleaned by conventional methods and dried. The capillaries were suspended over distilled water in an evacuated and sealed system. Approximately 18 hours or more were allowed for the formation of polywater in the tubes. Saturated salt solutions have also been used for obtaining the water vapor and for preparing samples. However, these were not used for the studies described below.

Infrared Spectra

Infrared spectra of polywater were obtained for samples both in and out of the tubes used for formation. For samples within the fused quartz tubes, the examination was limited to the

Dr. Lippincott is director of the Center for Materials Research and professor of chemistry at the University of Maryland, College Park. Dr. Stromberg is deputy chief of the polymers division of the Institute for Materials Research at National Bureau of Standards, Washington, D.C. Dr. Grant is a staff scientist of the polymer interface section at the National Bureau of Standards, Washington, D.C. Mr. Cessac is a predoctoral fellow in the department of chemistry at the University of Maryland, College Park.